Ag2V4O11: from primary to secondary battery

Etienne Le Calvez, Olivier Crosnier, Thierry Brousse

▶ **To cite this version:**

Etienne Le Calvez, Olivier Crosnier, Thierry Brousse. Ag2V4O11: from primary to secondary battery. Journal of Solid State Electrochemistry, 2022, 26 (9), pp.1951-1960. 10.1007/s10008-022-05224-9 . hal-04247592

HAL Id: hal-04247592
https://hal.science/hal-04247592

Submitted on 18 Oct 2023

HAL is a multi-disciplinary open access archive for the deposit and dissemination of scientific research documents, whether they are published or not. The documents may come from teaching and research institutions in France or abroad, or from public or private research centers.

L'archive ouverte pluridisciplinaire **HAL**, est destinée au dépôt et à la diffusion de documents scientifiques de niveau recherche, publiés ou non, émanant des établissements d'enseignement et de recherche français ou étrangers, des laboratoires publics ou privés.

$Ag_2V_4O_{11}$: from primary to secondary battery[z]

[z] Dedicated to Prof. Doron Aurbach, a researcher who genuinely investigated so many battery chemistries, providing major findings to our community.

Etienne Le Calvez[1,2], Olivier Crosnier[1,2], and Thierry Brousse[1,2]*

[1] Nantes Université, CNRS, Institut des Matériaux de Nantes Jean Rouxel, IMN, F-44000 Nantes, France

[2] Réseau sur le Stockage Electrochimique de l'Energie (RS2E), CNRS FR 3459, 33 rue Saint Leu, 80039 Amiens Cedex, France

Correspondence to: thierry.brousse@univ-nantes.fr

Keywords

Silver vanadate, sacrificial lithium salt, energy storage device, rechargeable Li-ion battery.

Abstract

$Ag_2V_4O_{11}$ (Silver Vanadium Oxide, SVO) is the positive electrode in primary Lithium/SVO batteries that had known an extraordinary success as a power source in implantable cardiac defibrillators (ICD). However, its use in rechargeable batteries is questioned due to the need of the negative lithium metal electrode that acts as the lithium source and that cannot be safely recharged in standard liquid electrolytes. In this study, a proof of concept of rechargeable graphite/SVO battery is demonstrated. The introduction of 3,4–dihydroxybenzonitrile dilithium salt (Li_2DHBN) as a sacrificial lithium source in the positive electrode allows *in situ* lithiation of the graphite electrode. The cell can further be cycled as a secondary battery. Different parameters have been investigated such as the particle size of $Ag_2V_4O_{11}$ synthesized by solid state and hydrothermal processes, especially with regards to peak power delivery. *In situ* XRD was used to investigate the link between irreversible silver reduction, which allows high electronic conductivity, and amorphization of the SVO structure.

Statements and Declarations

The authors disclose no financial interests that are directly or indirectly related to the work submitted for publication.

All authors contributed to the study conception and design. Conceptualization and Methodology were managed by T. Brousse and O. Crosnier. Material preparation, data collection and analyses were performed by E. Le Calvez and O. Crosnier. The first draft of the manuscript was written by E. Le Calvez and all authors commented on previous versions of the manuscript. All authors read and approved the final manuscript.

Introduction

Lithium/silver vanadium oxide ($Ag_2V_4O_{11}$, SVO) primary batteries have been developed from 1979.[1] Since then, they have met an outstanding commercial success mainly due to their ability to power implantable cardiac defibrillator (ICD) while meeting all the requirements of such peculiar application.[2] To summarize the major requirements expected for such batteries, it can be emphasized that an ICD continuously monitors heart function and on demand delivers a high-energy shock to the heart to treat arrhythmias. Practically, this means that apart from the continuous delivered current (10 to 50 µA) required to power the monitoring circuitry, there is a need to sustain high power pulses, in the range of 1 to 4 A, to rapidly charge the high voltage capacitors whose discharge to the heart interrupts the ventricular fibrillation. The Li/SVO battery is also able to be operated at 37°C (human body temperature) with less than 2% self-discharge per year on open-circuit storage or under low current drain. Long shell life is also depicted.[2] Moreover, a practical energy density close to 1000 Wh/L makes the Li/SVO system attractive for applications where battery size is of concern.

$Ag_2V_4O_{11}$ cathode of this primary battery and more largely the Li/SVO battery itself has been extensively studied by the team of Prof. Esther Takeuchi in numerous papers tackling all aspects of this energy storage device.[2–7] SVO cathode belongs to the class of vanadium bronzes and possesses semiconducting properties. Its electrochemical reduction is depicted as a multistep process taking place between 3.2 and 1.5 V vs Li^+/Li, leading to the overall reaction:

$$Ag_2V_4O_{11} + 7Li^+ + 7e^- \rightarrow Li_7Ag_2V_4O_{11} \quad (1)$$

This results in a theoretical capacity of 315 $mAh.g^{-1}$ within this potential window. The irreversible reduction of silver occurring at the highest potential of the electrochemical window, provides electronic conductivity to the surface of the SVO particles, which further enhances the high rate capability of this electrode. The growth of silver nanoparticles or nanowires upon the first stage of reduction has been evidenced by different teams.[8–10]

Although, Li/SVO batteries have been practically cycled over tenth of charge/discharge cycles, the use of the metallic lithium anode is detrimental to the safety of a practical use as rechargeable power source for ICD. This is indeed mainly related to the growth of lithium dendrites upon cycling at such temperatures, which can shortly lead to internal short-circuiting the battery.[11] However, with the growing interest in inductively rechargeable batteries, it can be great to design a SVO-based battery which keeps the advantages of this interesting cathode material. This supposes that a lithium source can be implemented in the battery and that this lithium reservoir is not supplied by a metallic lithium foil.

It can be noted that such a problematic is quite similar to that encountered by lithium-ion capacitors that are using a graphite-based negative electrode and an activated carbon positive electrode.[12–14] The lack of a lithium source is detrimental to the operation of such devices and practical solutions have been proposed to prelithiate the graphite anode during a preliminary charging step. These solutions are of three kinds: the use of a metallic lithium sacrificial electrode,[12] the use of the electrolyte as a lithium ions provider (at the expense of a decrease in ionic conductivity)[15] and the use of a lithium-rich sacrificial compound that can irreversibly provide lithium cations before becoming a dead weight in the battery.[16–18] This later solution has found some practical interest especially when molecules with high capacities are targeted.[19–23]

In this study, we propose to couple both approaches and provide a proof of concept of a graphite/ $Ag_2V_4O_{11}$ secondary battery. This will be achieved by mixing a lithiated organic material, namely 3,4–dihydroxybenzonitrile dilithium salt (Li_2DHBN) to $Ag_2V_4O_{11}$ positive electrode. This molecule will irreversibly provide lithium cations to a graphite electrode during an initial *in situ* charging step, while the graphite/ $Ag_2V_4O_{11}$ cell can be further cycled. Indeed, Li_2DHBN salt exhibits very interesting characteristics as a sacrificial lithium salt source in a Li-ion capacitor, with a high irreversible capacity (365 $mAh.g^{-1}$) which is delivered at a too high potential (<4.5V vs Li^+/Li) which prevents electrolyte decomposition. After delithiation, it dissolves in the electrolyte without gas formation, thus not altering the pressure in the cell. Moreover, the delithiated form of Li_2DHBN seems to be electrochemically inactive within a large potential window as demonstrated in our previous study.[23]

1. Experimental section

a. Synthesis of $Ag_2V_4O_{11}$ and Li_2DHBN

$Ag_2V_4O_{11}$ powders have been prepared by two distinct procedures. A solid-state synthesis method was used to synthesize $Ag_2V_4O_{11}$, further depicted as $Ag_2V_4O_{11}$ SS. Stoichiometric amounts of V_2O_5 (Alfa Aesar, 99.9% metal basis) and Ag_2O (ACROS Organics 99%) were thoroughly mixed using an agate mortar and pestle. The powdered mixture was heated at 550°C for 12 h in air using an alumina crucible. A hydrothermal method was also used to synthesize $Ag_2V_4O_{11}$ H. Stoichiometric amounts of V_2O_5 (Alfa Aesar, 99.9% metal basis) and $AgNO_3$ (ACROS Organics 99%) were introduced into a Teflon-lined vessel containing 15 mL of water. Then, 200 µL of ethylenediamine (Alfa Aesar) wereadded dropwise under stirring. After two hours, the vessels were introduced into their autoclaves and put in an oven at 180°C for 48h.

3,4-dihydroxybenzonitrile dilithium salt (Li_2DHBN) has been synthesized in a similar way to our previous report.[23] Briefly, 3,4-dihydroxybenzonitrile (Sigma-Aldrich) was introduced in a beaker which contained 14 mL of tetrahydrofuran in an oxygen free glove box. Then, LiH (Sigma-

Aldrich) was also introduced in order to start the ionic exchange between protons and lithium. After 15h of stirring, Li_2DHBN had totally precipitated and the powder was recovered by filtration and then dried under vacuum at 150°C.

b. Characterization

i. Powder X-ray diffraction

Powder XRD data were collected using a PANalytical X'Pert Pro diffractometer with a Cu source ($K_{\alpha1}$=1.5406Å, $K_{\alpha2}$=1.5444Å) and K_α filter (Nickel) in the Bragg-Brentano reflection geometry. Data were collected from 10 to 90° 2θ. *In situ* electrochemical cycling XRD patterns were obtained using a lab-produced cell, close to "Leriche cell" using a Beryllium window and by cycling the cell at 0.02 $A.g^{-1}$ with 30 min at open circuit voltage for XRD pattern acquisition.[24] All XRD were collected with ~0.008° 2θ steps.

ii. SEM

SEM micrographs were obtained using a Zeiss MERLIN Instrument operated at 20 kV using in-Lens annular detector. Samples were prepared by dispersing a small fraction of the powder on a piece of conducting carbon tape. EDX spectra were collected at 8.0 mm working distance using an X-Max 50 mm^2 OXFORD Instruments detector.

iii. Electrochemistry

To balance the mass ratio between $Ag_2V_4O_{11}$, Li_2DHBN and graphite, the electrode composition has been determined considering both the irreversible capacity of Li_2DHBN (365 $mAh.g^{-1}$) as well as the reversible capacity of graphite (around 370 $mAh.g^{-1}$) and $Ag_2V_4O_{11}$ (150 $mAh.g^{-1}$ which represents the capacity of $Ag_2V_4O_{11}$-H at 0.02 $A.g^{-1}$ as shown later). Then, mass ratio between Li_2DHBN and graphite was calculated to be 1.01. Mass ratio between $Ag_2V_4O_{11}$ and graphite was chosen as 2.46 in order to get the same capacity on the positive and negative electrode once the first lithiation has been performed. For these reasons, Li_2DHBN/$Ag_2V_4O_{11}$ electrode was fabricated with the ratio 1 Li_2DHBN: 2.50 $Ag_2V_4O_{11}$. The different freestanding electrodes are prepared following these compositions:

1) Li_2DHBN based electrode consisted of 45% of Li_2DHBN, 45% of conductive carbon and 10% of PTFE.

2) Positive electrode (Li_2DHBN with $Ag_2V_4O_{11}$ composite electrode) was fabricated following these proportions: 62.50% of $Ag_2V_4O_{11}$, 25.00% of Li_2DHBN, 6.25% of conducting carbon and 6.25% of polyvinylidene fluoride (PTFE) binder.

3) 89.00% of graphite, 1.00% of conducting carbon and 10.00% of PTFE were used for the fabrication of the freestanding negative electrode.

First, electrodes were prepared by thoroughly grinding the active material, conducting carbon (Superior graphite) and polyvinylidene fluoride (PTFE) binder (Sigma-Aldrich, 60 wt.% dispersion in H_2O) in a 75:15:10 wt. ratio, with about 2 mL of ethanol, until a homogeneous paste was obtained. Then, the paste was dried at 70°C overnight before introducing in glove box for incorporation of Li_2DHBN, as reported in our previous paper.[23] The latter was rolled out to a thickness of ~150 µm using a glass cylinder. Then, electrodes were cut into 12 mm diameter disks using a manual electrode puncher.

All the resulting electrode weights ranged between 5-10 $mg \cdot cm^{-2}$, consistent with reasonable mass loading.[25] Electrochemical experiments were performed using Swagelok®-type cells in a 2-electrode configuration. Cells were mounted inside an Argon-filled glovebox (<0.1 ppm O_2, H_2O) using a single Lithium (Li) foil as both the reference and counter electrode (99.9%, Sigma Aldrich). A glass fiber separator (Whatman) and 200 µL of 1 M $LiPF_6$ in ethylene carbonate/dimethyl carbonate (EC/DMC) 1:1 v/v (Solvionic, 99.9% purity, electrochemistry grade) were used as the separator and electrolyte, respectively. All electrochemical studies were performed using a MPG2 BioLogic Potentiostat/Galvanostat controlled by EC-Lab Software. Galvanostatic cycling with potential limitation (GCPL) was performed in a series of 5 cycles at 0.02, 0.05, 0.10, 0.20, 0.50, 1.00 and 2.00 $A \cdot g^{-1}$ (considering mass of active materials) between 1.5V and 3.2V vs Li^+/Li. The charge-discharge plots shown in the related figures always correspond to the third charge/discharge cycle.

2. Results & Discussion

In this work, we revisited the electrochemistry of $Ag_2V_4O_{11}$ not only as primary lithium-ion battery cathode materials but also as active materials in positive electrodes for rechargeable batteries. For these reasons, two different syntheses have been performed to compare the influence of particle size on lithium ions intercalation.

$Ag_2V_4O_{11}$ has a monoclinic structure (space group C2/m) with cell parameters close to a= 15.48 Å, b= 3.58 Å, c= 9.58 Å and β= 128.74 Å.[26] The layered structure of this oxide is formed by 2x2 edge-sharing highly distorted octahedra that are linked together by corner-sharing, as presented in Figure 1. These layers are formed along the *a* axis. Between these $(V_4O_{12})_n$ layers, silver cations (Ag^+) are coordinated with 7 oxygen atoms. In fact, the stability of these layers seems to be possible thanks to the sharing of some octahedral by their edges.[27] The structure is very close to $Cu_{1.8}V_4O_{11}$ as pointed out by Rozier *et al.* [9] $Ag_2V_4O_{11}$ has been considered in the past as a possible electrode material for high power primary lithium ions batteries due to its layered structure as well as the possible reduction of both silver and vanadium cations during the discharge as previously explained. Indeed, silver nanoparticles help to increase the electronic conductivity of the electrode.

As presented in Figure 2.A, XRD patterns show that a pure phase is obtained with both syntheses. All the main reflections peaks of the phase are visible between 20 and 60°. Furthermore, a large difference in terms of crystallite size is observed, as it can be seen with the much broader peaks observed in the case of $Ag_2V_4O_{11}$ H. In fact, the average crystallite size is found to be > 1 µm in the case of solid-state synthesis and ~250 nm in the case of hydrothermal synthesis. These results are found by applying the Scherrer equation on (110) and (003) peaks.

SEM images at different magnifications are presented in Figure 2.(B-E). Both types of particles presented preferential growth along $[30\bar{2}]$ with rods like shape. [28-29] Nevertheless, particles size is found to be much smaller in the case of $Ag_2V_4O_{11}$ - H as expected from XRD patterns: particles synthesized using solid-state synthesis exhibit a size of a few tens of micrometers, while hydrothermal particles are nanorods of about 500 nm long with a diameter of 50 nm. Moreover, these nanorods are agglomerated and form micrometer size secondary particles.

Thanks to the large difference in terms of crystallite and particle size between hydrothermal and solid-state reactions, it is of interest to compare the respective electrochemical responses of both materials *vs* a lithium metal electrode. For this reason, charge-discharge cycles at different current densities have been performed. The results are presented in Figure 3.(A-B). To avoid the re-oxidation of Ag^0 to Ag^+ the potential should not exceed 3.2V upon oxidation sweep.[6,7] Thus, the selected potential range of the experiment has been set up between 1.5V and 3.2V vs Li^+/Li. During the first reduction, capacities are 277 $mAh.g^{-1}$ and 292 $mAh.g^{-1}$ for respectively solid-state and hydrothermal $Ag_2V_4O_{11}$ electrodes. These values correspond to the insertion of respectively 6.1 and 6.5 $Li^+/Ag_2V_4O_{11}$. This large capacity during the first reduction is assigned to both silver reduction which allows Ag^+/Li^+ displacement reaction (Equation 2) and V^{5+}/V^{4+} reduction followed by the partial reduction of V^{4+} into V^{3+} (Equation 3). The charge storage mechanism of this first reduction will be discussed later. The low coulombic efficiency of the first cycle is also explained by the irreversible reduction of Ag^+ to metallic silver and then part of the Li^+ needs to remain in the interlayer to prevent the collapsing of the pristine layered structure.

$$Ag_2V_4O_{11} + xLi^+ + 2e^- \rightarrow Li_xV_4O_{11} + 2Ag^0 \qquad \text{with } x < 2 \qquad (2)$$

$$Li_xV_4O_{11} + yLi^+ + ye^- \rightarrow Li_{x+y}V_4O_{11} \qquad \text{with } y < 5 \qquad (3)$$

After this first cycle, both materials presented a relatively high reversible capacity between 1.5V-3.2V vs Li^+/Li. At a current density of 0.02 $A.g^{-1}$, a capacity of around 150 $mAh.g^{-1}$ is observed for the electrodes prepared using both $Ag_2V_4O_{11}$ powders. This capacity represented 3.3 $Li^+/Ag_2V_4O_{11}$. However, when the current density increases, a faster decrease in the capacity retention is observed for $Ag_2V_4O_{11}$ – SS sample compared to $Ag_2V_4O_{11}$ - H. For example, at 0.10 $A.g^{-1}$ and 0.50 $A.g^{-1}$, $Ag_2V_4O_{11}$ – SS exhibits respectively 78 and 14 $mAh.g^{-1}$ while $Ag_2V_4O_{11}$ - H shows 109 and 73 $mAh.g^{-1}$. A smaller lithium diffusion pathway that limits the intrinsic kinetic limitations of this phase

can explain this better capacity retention. In fact, Fick's first law concerning diffusion explained that diffusion length has a strong impact on diffusion time. ($L \propto \sqrt{D.t}$ where L is the diffusion length, D, is the diffusion coefficient and t, is the diffusion time).

Figure 3.D shows the cyclability of both powders at 0.2 $A.g^{-1}$upon cycling. After 250 cycles and considering the second cycle as the reference, capacity retentions of about 75% and 110% are observed for solid-state and hydrothermal $Ag_2V_4O_{11}$, respectively. It can be noticed that the capacity increases after few cycles in the case of $Ag_2V_4O_{11}$-H, which can be due to a continuous change of the structure during these first cycles allowing a greater insertion of the lithium ions. From our understanding, nanomaterials undergo lower stress which leads to a better capacity retention upon cycling.

To understand more in-depth the charge storage mechanism occurring in $Ag_2V_4O_{11}$-H, *in situ* XRD experiments were performed at 0.02 $A.g^{-1}$ between 1.5 and 3.2V *vs* Li^+/Li during the first reduction. In 2010, Sauvage *et al.*. carried out in-depth *in situ* XRD characterizations on micrometric $Ag_2V_4O_{11}$.[32] They found that at the early stage of the lithiation, Li^+ insertion occurs without Ag^+ displacement and/or reduction. For this reason, no amorphization takes place. However, after the insertion of around one lithium per chemical formula, a progressive loss of crystallinity occurs in parallel to silver reduction until full amorphization at 2.2 Li^+ per chemical formula. Then, steady reduction of silver continues until reaching a fully metallic silver state. *In situ* XRD experiment of $Ag_2V_4O_{11}$ - H is represented in Figure 4(A-B-C). It is found that both amorphization and silver reduction take place at the beginning of the lithiation. In the case of $Ag_2V_4O_{11}$-H, Li^+/Ag^+ displacement reaction occurs at the first stage of the reduction process and not V^{5+}/V^{4+} reduction. The reaction is in this sense dependent of particle size, which is in agreement with literature data.[31] The collapse of the structure can be explained by the bigger ionic radii of silver cations (1.22 Å) compared to Li^+ ions (0.76 Å) which does not allow the layer architecture to be stable.[9, 10] Furthermore, the reduction of silver creates nanoparticles of metallic silver at the surface of $Li_xAg_{2-y}V_4O_{11}$ (x<y) particles. This "coating" has been reported to increase the electronic conductivity and then allows its use as high power primary cathode material.[33-35]

Then, after the characterization of $Ag_2V_4O_{11}$ with two different morphologies, the next step was to show that this lithium-free oxide could be used in association with a sacrificial lithium source in a secondary lithium-ion battery setup. In other words, the idea of the present paper is summarized in Figure 5.A. Here, $Ag_2V_4O_{11}$ - H will be used as efficient negative electrode materials. Moreover, Li_2DHBN was considered as a source of lithium as it shows a relevant behavior in Li-ion capacitor.[23]

First, two different electrodes have been prepared, one serving as the reference with only 3,4–dihydroxybenzonitrile dilithium salt (Li_2DHBN) and a second one which is a composite of $Ag_2V_4O_{11}$

and Li_2DHBN. Details on the mass ratio between $Ag_2V_4O_{11}$ and Li_2DHBN can be found in the experimental section. To provide lithium to the system, the irreversible delithiation of Li_2DHBN occurs between 3.0V and 4.0V vs Li^+/Li. This delithiation has been performed using a charging rate of C/10 considering the mass of Li_2DHBN. As shown in Figure 5.B, the delithiation behavior of the pristine Li_2DHBN and the composite positive electrodes is similar with a capacity of about 300 $mAh.g^{-1}$ (per g of Li_2DHBN). This capacity translates in a release of 1.7 Li^+/Li_2DHBN. The difference in terms of delithiation potential is due to the larger open circuit potential of the composite electrode containing $Ag_2V_4O_{11}$ - H and Li_2DHBN. We can then conclude that delithiation of Li_2DHBN occurs in a similar manner with or without the presence of $Ag_2V_4O_{11}$ - H.

After this irreversible delithiation of the Li_2DHBN organic molecule, DHBN is dissolved in electrolyte and not present anymore in the positive electrode as explained by P. Jezowski *et al.*[23] Figure 5.C reports on the following cycles at different current densities when metallic lithium is used as the negative electrode. As observed, $Ag_2V_4O_{11}$ - H presents a discharge capacity on the third cycle of 120 $mAh.g^{-1}$ at 0.02 $A.g^{-1}$ between 3.2V and 1.5V vs Li^+/Li. Compared to the Li_2DHBN-free $Ag_2V_4O_{11}$ - H electrode (Figure 3.B), we observed a decrease of 40 $mAh.g^{-1}$, which is mainly due to vanadium dissolution during first Li_2DHBN delithiation. [38] In fact, the separator is found to be greenish, which is characteristic of V^{5+} species in solution. The following cycles show good capacity retention indicating that $Ag_2V_4O_{11}$ dissolution only occurs concomitantly with this initial delithiation. At 0.05 and 0.1 $A.g^{-1}$, the values of capacity are equal to 63 and 33 $mAh.g^{-1}$ respectively (Figure 5.C). These lower capacities compared to the pristine Li_2DHBN-free $Ag_2V_4O_{11}$ - H electrode (Figure 3.B) can be explained by several reasons. First, the ratio between $Ag_2V_4O_{11}$ and conductive carbon has not been optimized in Li_2DHBN $Ag_2V_4O_{11}$ - H electrode with a low amount of conductive carbon (6.25%). In fact, adding more conductive carbon can increase the electronic conductivity of the electrode and then improve the capacity at higher current densities. Furthermore, the electronic percolation can be deteriorated by the dissolution of Li_2DHBN in the electrode. Nevertheless, we note that the electrode works relatively well at moderate current densities. For this reason, the Li_2DHBN $Ag_2V_4O_{11}$ - H composite electrode has been further associated with a graphite negative electrode in a full device assembly.

The two first cycles of the Li_2DHBN $Ag_2V_4O_{11}$ - H electrode *vs* a graphite electrode are presented Figure 5.(D-E). A thick lithium wire has been used to monitor the evolution of both electrode potentials. During the first charge, at the positive electrode, Li_2DHBN effectively releases its lithium cations (around 1.8 Li^+/Li_2DHBN), thus evidencing the effectiveness of *in situ* lithiation of the cell. In the negative electrode, graphite inserts lithium cations until reaching ~0.1V vs Li^+/Li as typically observed for this negative electrode material that has been deeply investigated by Prof. Doron Aurbach and his team.[36–38] The observed capacity is about 350 $mAh.g^{-1}$, which is very close to its theoretical capacity of 372 $mAh.g^{-1}$. Moreover, the plateau observed at ~0.8V vs Li^+/Li represents the

formation of the solid electrolyte interphase (SEI). During the second discharge, the cell shows a relatively poor coulombic efficiency with less than 40%. In fact, the graphite electrode only partially releases the inserted lithium. Several explanations can support this poor coulombic efficiency. First of all, the vanadium which is liberated and dissolved during the Li_2DHBN delithiation can further react during the SEI formation and/or migrate to the anode and simply be deposited on the surface of the graphite electrode as observed by Takeuchi.[39-40] This has been largely commented in literature concerning Mn^{2+} dissolution in $LiMn_2O_4$ and is responsible for similar issues.[41–43] As well, silver metal and/or silver ions can also be dissolved, and migrate to the graphite electrode giving rise to this poor coulombic efficiency. [40-41] Lastly, it is also possible that the delithiated DHBN molecules are involved in the complexation of vanadium species in solution, thus disturbing the formation of the SEI on the surface of graphite, and then partially preventing the lithium ions from leaving the graphite upon subsequent discharge of the cell. As observed in Figure 5.E, the coulombic efficiency is still poor for the following cycle. Based on the literature data, different solutions can be used to increase the coulombic efficiency. Among them, using high concentrated salt and/or adding additives in the electrolyte can reduce vanadium dissolution.[42,44-45] Carbon-coated $Ag_2V_4O_{11}$ particles can also allow to cancel this drawback.[48] These solutions are currently under investigation to obtain a better coulombic efficiency. Nevertheless, this first insight of how to turn $Ag_2V_4O_{11}$/Li primary battery into $Ag_2V_4O_{11}$/graphite secondary (rechargeable) battery has been demonstrated, thanks to *in situ* lithiation of this system using Li_2DHBN sacrificial molecules. This work provides new guidelines to use non-lithiated positive electrodes in rechargeable lithium ion-batteries.

Conclusion

This work presents the characterization of two $Ag_2V_4O_{11}$ powders synthesized by solid-state and hydrothermal processes. Hydrothermal $Ag_2V_4O_{11}$ exhibits superior electrochemical behavior with a capacity of 150 $mAh.g^{-1}$ at a moderate current density (0.02 $A.g^{-1}$) between 1.5V and 3.0V vs Li^+/Li after an initial capacity of 300 $mAh.g^{-1}$. *In situ* XRD has shown the irreversible reduction of silver during the first cycle concomitantly to the amorphization of the structure. Moreover, $Ag_2V_4O_{11}$ - H was associated to a sacrificial organic lithium salt at the positive electrode and the related composite electrode was tested against graphite as negative electrodes in rechargeable batteries. This is a first report of such a proof of concept of how to turn a performing positive electrode for primary batteries into a rechargeable cathode for a lithium-ion cell. In this study, we highlighted the possibility of using such a device even if coulombic efficiency is still modest for this first insight. Finally, several other possibilities exist for improving the system and potentially achieve better coulombic efficiency, especially with the use of other sacrificial salts (Li_3N, $Li_2C_4O_4$…).[19-22, 50–51]

Acknowledgements

Authors would like to thanks Pawel Jezowski (Poznan University of Technology) for the synthesis of Li_2DHBN powder and for fruitful discussions. Marion Allart is deeply thanked for SEM observations and EDX analyses. The authors would like to acknowledge Nantes Université/NExT program (ANR-16-IDEX-0007, DISCUSS project) and Labex STORE-EX (ANR-10-LABX-76-01) for financial support.

Figures

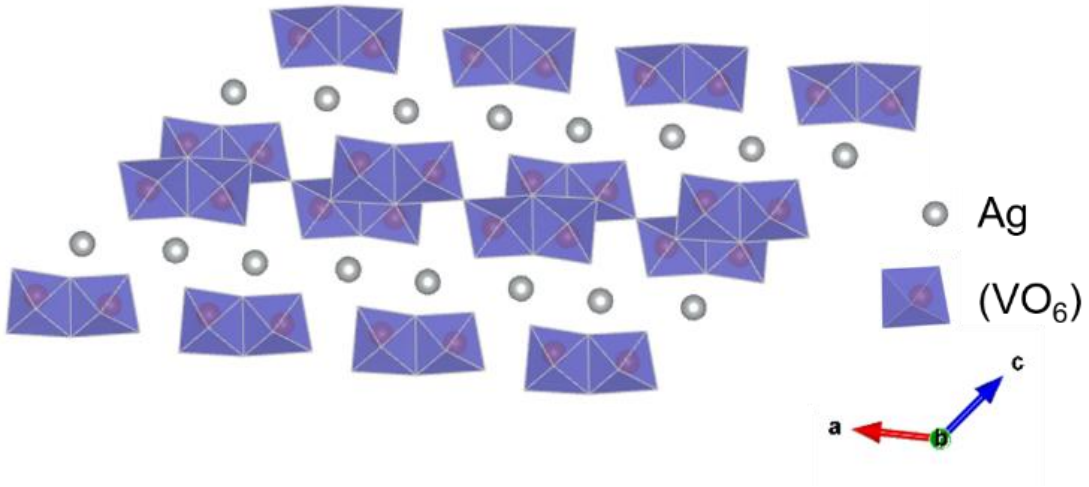

Figure 1. A Crystal structure of $Ag_2V_4O_{11}$

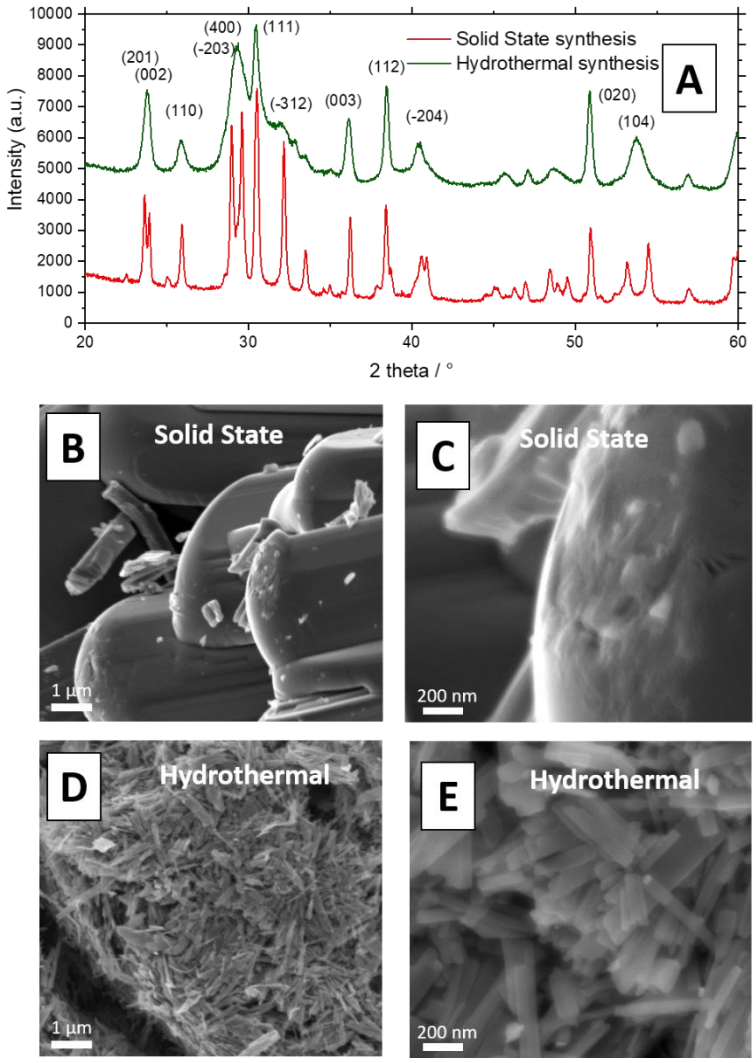

Figure 2. (A) Diffractograms of $Ag_2V_4O_{11}$ synthesized by solid state and hydrothermal method **(B-C).** SEM images of $Ag_2V_4O_{11}$ synthesized by solid-state method. **(D-E).** SEM images of $Ag_2V_4O_{11}$ synthesized by hydrothermal method.

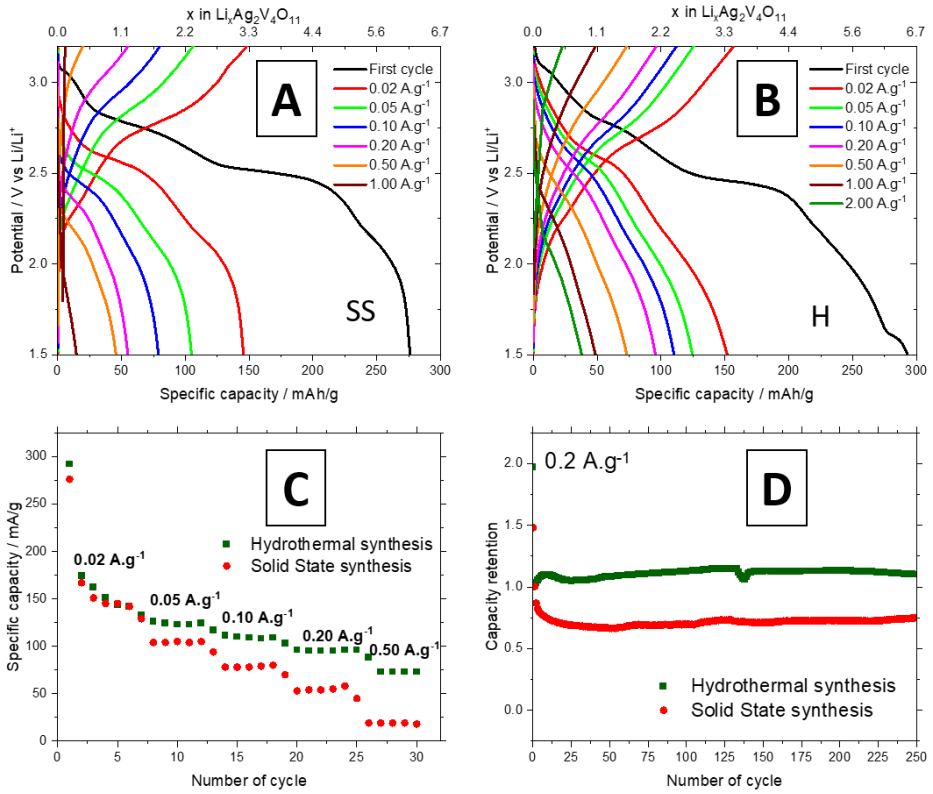

322

323 **Figure 3. (A-B).** Charge-discharge experiments at different current densities for $Ag_2V_4O_{11}$ synthesized
324 by hydrothermal method. **(C).** Specific capacity *vs* cycle number at different current densities for both
325 solid state and hydrothermal powders. **(D).** Cycling stability of both $Ag_2V_4O_{11}$ synthesized by solid
326 state and hydrothermal methods.

327

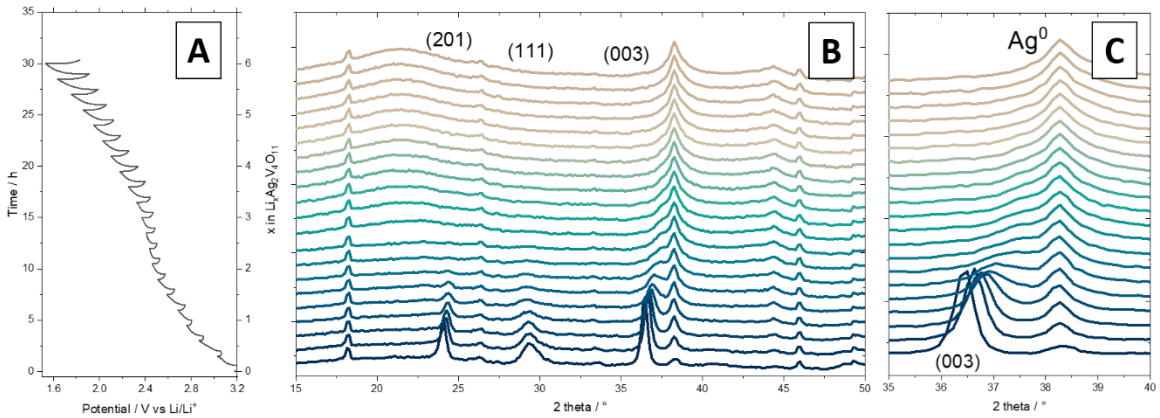

328

329 **Figure 4.** *In situ* XRD experiment of $Ag_2V_4O_{11}$ synthesized by hydrothermal method. **(A)** First
330 discharge curve at 0.05 $A.g^{-1}$ **(B-C)** Associated diffractograms of $Ag_2V_4O_{11}$ at different states of
331 discharge.

332

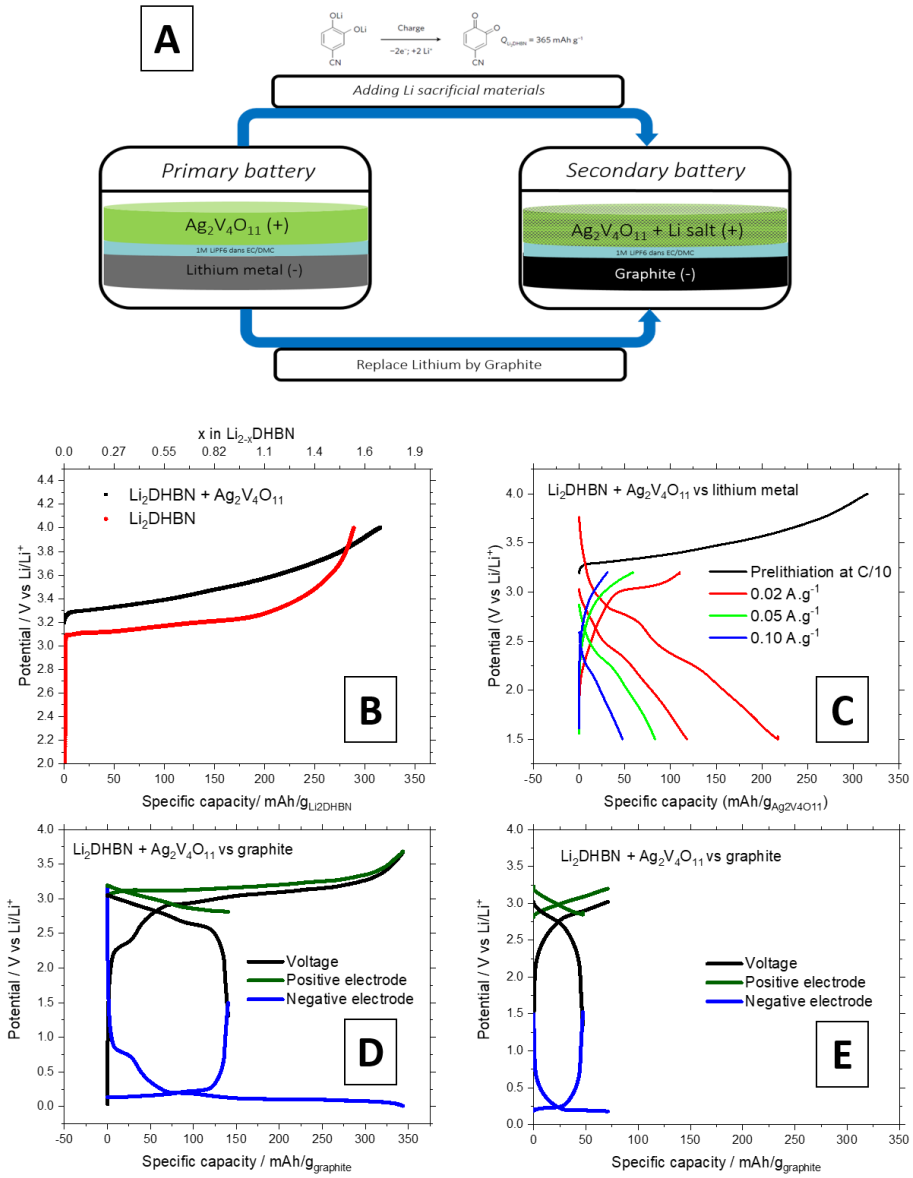

Figure 5. (A) Scheme of the proposed transition from a primary battery to a secondary and therefore rechargeable battery using a sacrificial salt and $Ag_2V_4O_{11}$. **(B)** Electrochemical delithiation of Li_2DHBN associated or not with $Ag_2V_4O_{11}$ at a charging rate of C/10 (considering the theoretical capacity of Li_2DHBN). **(C)** Charge and discharge plots of $Ag_2V_4O_{11}$ with Li_2DHBN at different current densities vs metallic lithium. **(D)** First cycle of $Ag_2V_4O_{11}$ with Li_2DHBN associated with a graphite electrode at C/5 (considering the mass of graphite). **(E)** Second cycle of $Ag_2V_4O_{11}$ with Li_2DHBN associated with a graphite electrode at C/5 (considering mass of graphite).

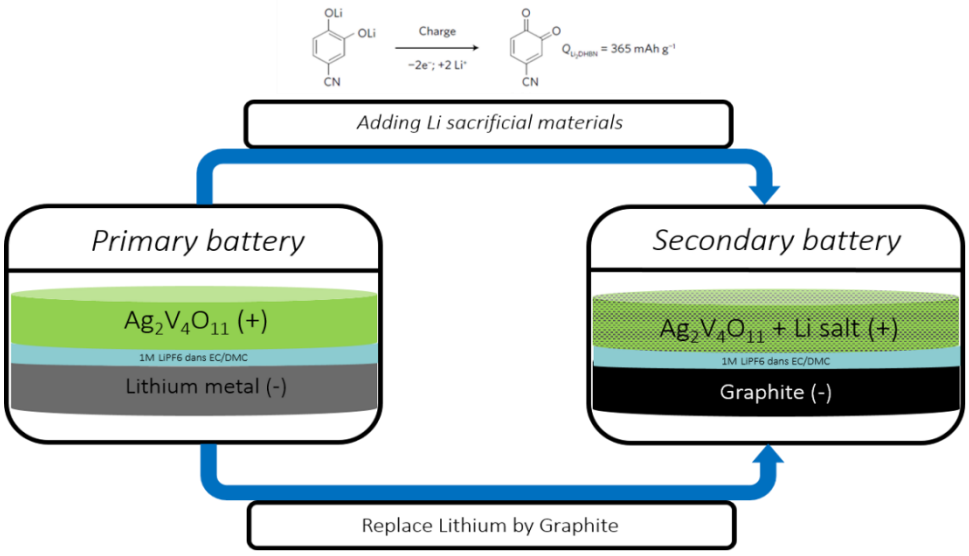

Graphical abstract

Bibliography

[1] C. C. Liang, M. E. Bolster, et R. M. Murphy, *Metal oxide composite cathode material for high energy density batteries*. Google Patents, 1983.

[2] E. S. Takeuchi et W. C. Thiebolt, « The reduction of silver vanadium oxide in lithium/silver vanadium oxide cells », *J. Electrochem. Soc.*, vol. 135, n° 11, p. 2691, 1988.

[3] D. C. Bock, K. J. Takeuchi, A. C. Marschilok, et E. S. Takeuchi, « Silver vanadium oxide and silver vanadium phosphorous oxide dissolution kinetics: a mechanistic study with possible impact on future ICD battery lifetimes », *Dalton Trans.*, vol. 42, n° 38, p. 13981‑13989, 2013.

[4] G. M. Bergman, S. J. Ebel, E. S. Takeuchi, et P. Keister, « Heat dissipation from lithium/silver vanadium oxide cells during storage and low-rate discharge », *J Power Sources Switzerland*, vol. 20, n° 3/4, 1987.

[5] E. S. Takeuchi et P. Piliero, « Lithium/silver vanadium oxide batteries with various silver to vanadium ratios », *J Power Sources Switzerland*, vol. 21, n° 2, 1987.

[6] D. C. Bock, A. C. Marschilok, K. J. Takeuchi, et E. S. Takeuchi, « A kinetics and equilibrium study of vanadium dissolution from vanadium oxides and phosphates in battery electrolytes: Possible impacts on ICD battery performance », *J. Power Sources*, vol. 231, p. 219‑225, 2013.

[7] N. D. Leifer *et al.*, « Nuclear magnetic resonance and X-ray absorption spectroscopic studies of lithium insertion in silver vanadium oxide cathodes », *J. Electrochem. Soc.*, vol. 154, n° 6, p. A500, 2007.

[8] M. Morcrette *et al.*, « A reversible copper extrusion–insertion electrode for rechargeable Li batteries », *Nat. Mater.*, vol. 2, n° 11, p. 755‑761, 2003.

[9] K. West et A. M. Crespi, « Lithium insertion into silver vanadium oxide, $Ag_2V_4O_{11}$ », *J. Power Sources*, vol. 54, n° 2, p. 334‑337, 1995.

[10] F. Sauvage, V. Bodenez, J.-M. Tarascon, et K. R. Poeppelmeier, « Room-temperature synthesis leading to nanocrystalline $Ag_2V_4O_{11}$ », *J. Am. Chem. Soc.*, vol. 132, n° 19, p. 6778‑6782, 2010.

[11] D. Aurbach, E. Zinigrad, Y. Cohen, et H. Teller, « A short review of failure mechanisms of lithium metal and lithiated graphite anodes in liquid electrolyte solutions », *Solid State Ion.*, vol. 148, n° 3‑4, p. 405‑416, 2002.

[12] T. Aida, K. Yamada, et M. Morita, « An advanced hybrid electrochemical capacitor that uses a wide potential range at the positive electrode », *Electrochem. Solid-State Lett.*, vol. 9, n° 12, p. A534, 2006.

[13] G. G. Amatucci, F. Badway, A. Du Pasquier, et T. Zheng, « An asymmetric hybrid nonaqueous energy storage cell », *J. Electrochem. Soc.*, vol. 148, n° 8, p. A930, 2001.

[14] K. Naoi, S. Ishimoto, J. Miyamoto, et W. Naoi, « Second generation ‘nanohybrid supercapacitor’: evolution of capacitive energy storage devices », *Energy Environ. Sci.*, vol. 5, n° 11, p. 9363‑9373, 2012.

[15] C. Decaux, G. Lota, E. Raymundo-Piñero, E. Frackowiak, et F. Béguin, « Electrochemical performance of a hybrid lithium-ion capacitor with a graphite anode preloaded from lithium bis (trifluoromethane) sulfonimide-based electrolyte », *Electrochimica Acta*, vol. 86, p. 282‑286, 2012.

[16] M.-S. Park, Y.-G. Lim, J.-H. Kim, Y.-J. Kim, J. Cho, et J.-S. Kim, « A Novel Lithium‐Doping Approach for an Advanced Lithium Ion Capacitor », *Adv. Energy Mater.*, vol. 1, n° 6, p. 1002‑1006, 2011.

[17] P. Jeżowski, K. Fic, O. Crosnier, T. Brousse, et F. Béguin, « Lithium rhenium (vii) oxide as a novel material for graphite pre-lithiation in high performance lithium-ion capacitors », *J. Mater. Chem. A*, vol. 4, n° 32, p. 12609‑12615, 2016.

[18] P. Jeżowski, K. Fic, O. Crosnier, T. Brousse, et F. Béguin, « Use of sacrificial lithium nickel oxide for loading graphitic anode in Li-ion capacitors », *Electrochimica Acta*, vol. 206, p. 440‑445, 2016.

[19] M. Arnaiz *et al.*, « A transversal low-cost pre-metallation strategy enabling ultrafast and stable metal ion capacitor technologies », *Energy Environ. Sci.*, vol. 13, n° 8, p. 2441‑2449, 2020.

[20] B. Anothumakkool, S. Wiemers‐Meyer, D. Guyomard, M. Winter, T. Brousse, et J. Gaubicher, « Cascade‐Type Prelithiation Approach for Li‐Ion Capacitors », *Adv. Energy Mater.*, vol. 9, n° 27, p. 1900078, 2019.

[21] D. Shanmukaraj, S. Grugeon, S. Laruelle, G. Douglade, J.-M. Tarascon, et M. Armand, « Sacrificial salts: compensating the initial charge irreversibility in lithium batteries », *Electrochem. Commun.*, vol. 12, n° 10, p. 1344‑1347, 2010.
[22] M. Arnaiz et J. Ajuria, « Pre-Lithiation Strategies for Lithium Ion Capacitors: Past, Present, and Future », *Batter. Supercaps*, vol. 4, n° 5, p. 733‑748, 2021.
[23] P. Jeżowski, O. Crosnier, E. Deunf, P. Poizot, F. Béguin, et T. Brousse, « Safe and recyclable lithium-ion capacitors using sacrificial organic lithium salt », *Nat. Mater.*, vol. 17, n° 2, p. 167‑173, 2018.
[24] J. B. Leriche *et al.*, « An Electrochemical Cell for Operando Study of Lithium Batteries Using Synchrotron Radiation », *J. Electrochem. Soc.*, vol. 157, n° 5, p. A606, 2010, doi: 10.1149/1.3355977.
[25] Y. Gogotsi et P. Simon, « True Performance Metrics in Electrochemical Energy Storage », *Science*, vol. 334, n° 6058, p. 917, nov. 2011, doi: 10.1126/science.1213003.
[26] M. Onoda et K. Kanbe, « Crystal structure and electronic properties of the $Ag_2V_4O_{11}$ insertion electrode », *J. Phys. Condens. Matter*, vol. 13, n° 31, p. 6675, 2001.
[27] B. Raveau, « Structural relationships in lamellar oxides build up from edge-sharing octahedra », *Rev. Inorg. Chem.*, vol. 9, n° 1, p. 37‑64, 1987.
[28] H. Shi, Z. Li, J. Kou, J. Ye, et Z. Zou, « Facile synthesis of single-crystalline $Ag_2V_4O_{11}$ nanotube material as a novel visible-light-sensitive photocatalyst », *J. Phys. Chem. C*, vol. 115, n° 1, p. 145‑151, 2011.
[29] G. Shen et D. Chen, « Self-coiling of $Ag_2V_4O_{11}$ nanobelts into perfect nanorings and microloops », *J. Am. Chem. Soc.*, vol. 128, n° 36, p. 11762‑11763, 2006.
[30] E. S. Takeuchi et W. C. Thiebolt, « The reduction of silver vanadium oxide in lithium/silver vanadium oxide cells », *J. Electrochem. Soc.*, vol. 135, n° 11, p. 2691, 1988.
[31] F. Sauvage, V. Bodenez, J.-M. Tarascon, et K. R. Poeppelmeier, « Room-temperature synthesis leading to nanocrystalline $Ag_2V_4O_{11}$ », *J. Am. Chem. Soc.*, vol. 132, n° 19, p. 6778‑6782, 2010.
[32] F. Sauvage, V. Bodenez, H. Vezin, M. Morcrette, J.-M. Tarascon, et K. R. Poeppelmeier, « Structural and transport evolution in the $Li_xAg_2V_4O_{11}$ system », *J. Power Sources*, vol. 195, n° 4, p. 1195‑1201, 2010.
[33] R. D. Shannon et C. T. Prewitt, « Effective ionic radii in oxides and fluorides », *Acta Crystallogr. Sect. B*, vol. 25, n° 5, p. 925‑946, mai 1969, doi: 10.1107/S0567740869003220.
[34] R. D. Shannon, « Revised effective ionic radii and systematic studies of interatomic distances in halides and chalcogenides », *Acta Crystallogr. Sect. A*, vol. 32, n° 5, p. 751‑767, sept. 1976, doi: 10.1107/S0567739476001551.
[35] E. S. Takeuchi, A. C. Marschilok, K. Tanzil, E. S. Kozarsky, S. Zhu, et K. J. Takeuchi, « Electrochemical Reduction of Silver Vanadium Phosphorus Oxide, $Ag_2VO_2PO_4$: The Formation of Electrically Conductive Metallic Silver Nanoparticles », *Chem. Mater.*, vol. 21, n° 20, p. 4934‑4939, 2009.
[36] K. C. Kirshenbaum, D. C. Bock, A. B. Brady, A. C. Marschilok, K. J. Takeuchi, et E. S. Takeuchi, « Electrochemical reduction of an $Ag_2VO_2PO_4$ particle: dramatic increase of local electronic conductivity », *Phys. Chem. Chem. Phys.*, vol. 17, n° 17, p. 11204‑11210, 2015.
[37] K. Kirshenbaum *et al.*, « In situ visualization of $Li/Ag_2VP_2O_8$ batteries revealing rate-dependent discharge mechanism », *Science*, vol. 347, n° 6218, p. 149‑154, 2015.
[38] R. DeMayo, D. C. Bock, K. J. Takeuchi, A. C. Marschilok, et E. S. Takeuchi, « Cathode Dissolution as a Battery Failure Mechanism in Silver Vanadium Oxide (SVO) and Structurally-Stabilized SVO-Analogue Materials Using Phosphate (PO_4^{3-}) », *ECS Trans.*, vol. 66, n° 9, p. 231, 2015.
[39] D. Aurbach *et al.*, « Common electroanalytical behavior of Li intercalation processes into graphite and transition metal oxides », *J. Electrochem. Soc.*, vol. 145, n° 9, p. 3024, 1998.
[40] D. Aurbach, H. Teller, M. Koltypin, et E. Levi, « On the behavior of different types of graphite anodes », *J. Power Sources*, vol. 119, p. 2‑7, 2003.
[41] B. Markovsky, M. D. Levi, et D. Aurbach, « The basic electroanalytical behavior of practical graphite–lithium intercalation electrodes », *Electrochimica Acta*, vol. 43, n° 16‑17, p. 2287‑2304, 1998.

[42] D. C. Bock, K. J. Takeuchi, A. C. Marschilok, et E. S. Takeuchi, « Structural and silver/vanadium ratio effects on silver vanadium phosphorous oxide solution formation kinetics: Impact on battery electrochemistry », *Phys. Chem. Chem. Phys.*, vol. 17, n° 3, p. 2034‑ 2042, 2015.

[43] Y. Liu, J. Lv, Y. Fei, X. Huo, et Y. Zhu, « Improvement of storage performance of $LiMn_2O_4$/graphite battery with AlF_3-coated $LiMn_2O_4$ », *Ionics*, vol. 19, n° 9, p. 1241‑ 1246, sept. 2013, doi: 10.1007/s11581-013-0853-x.

[44] R. Wang, X. Li, Z. Wang, et H. Guo, « Manganese dissolution from $LiMn_2O_4$ cathodes at elevated temperature: methylene methanedisulfonate as electrolyte additive », *J. Solid State Electrochem.*, vol. 20, n° 1, p. 19‑ 28, janv. 2016, doi: 10.1007/s10008-015-2998-1.

[45] Y. Tesfamhret, H. Liu, Z. Chai, E. Berg, et R. Younesi, « On the Manganese Dissolution Process from $LiMn_2O_4$ Cathode Materials », *ChemElectroChem*, vol. 8, n° 8, p. 1516‑ 1523, avr. 2021, doi: 10.1002/celc.202001496.

[46] N. Dubouis *et al.*, « Extending insertion electrochemistry to soluble layered halides with superconcentrated electrolytes », *Nat. Mater.*, vol. 20, n° 11, p. 1545‑ 1550, 2021.

[47] S. Komaba, B. Kaplan, T. Ohtsuka, Y. Kataoka, N. Kumagai, et H. Groult, « Inorganic electrolyte additives to suppress the degradation of graphite anodes by dissolved Mn(II) for lithium-ion batteries », *Sel. Pap. Present. 11th Int. Meet. Lithium Batter.*, vol. 119‑ 121, p. 378‑ 382, juin 2003, doi: 10.1016/S0378-7753(03)00224-6.

[48] J. Wang *et al.*, « Surface aging at olivine $LiFePO_4$: a direct visual observation of iron dissolution and the protection role of nano-carbon coating », *J. Mater. Chem. A*, vol. 1, n° 5, p. 1579‑ 1586, 2013, doi: 10.1039/C2TA00521B.

[50] C. Sun, X. Zhang, C. Li, K. Wang, X. Sun, et Y. Ma, « High-efficiency sacrificial prelithiation of lithium-ion capacitors with superior energy-storage performance », *Energy Storage Mater.*, vol. 24, p. 160‑ 166, 2020.

[51] K. Zou *et al.*, « Molecularly Compensated Pre‑ Metallation Strategy for Metal‑ Ion Batteries and Capacitors », *Angew. Chem. Int. Ed.*, vol. 60, n° 31, p. 17070‑ 17079, 2021.